Int J CARS (2015) 10:253–262
DOI 10.1007/s11548-014-1110-0

ORIGINAL ARTICLE

Electromagnetic tracking in surgical and interventional environments: usability study

Elodie Lugez · Hossein Sadjadi · David R. Pichora · Randy E. Ellis · Selim G. Akl · Gabor Fichtinger

Received: 23 April 2014 / Accepted: 10 August 2014 / Published online: 6 September 2014

Abstract
Purpose Electromagnetic (EM) tracking of instruments within a clinical setting is notorious for fluctuating measurement performance. Position location measurement uncertainty of an EM system was characterized in various environments, including control, clinical, cone beam computed tomography (CBCT), and CT scanner environments. Static and dynamic effects of CBCT and CT scanning on EM tracking were evaluated.
Methods Two guidance devices were designed to solely translate or rotate the sensor in a non-interfering fit to decouple pose-dependent tracking uncertainties. These devices were mounted on a base to allow consistent and repeatable tests when changing environments. Using this method, position and orientation measurement accuracies, precision, and 95 % confidence intervals were assessed.
Results The tracking performance varied significantly as a function of the environment—especially within the CBCT and CT scanners—and sensor pose. In fact, at a fixed sensor position in the clinical environment, the measurement error varied from 0.2 to 2.2 mm depending on sensor orientations. Improved accuracies were observed along the vertical axis of the field generator. Calibration of the measurements improved tracking performance in the CT environment by 50–85 %.
Conclusion EM tracking can provide effective assistance to surgeons or interventional radiologists during procedures performed in a clinical or CBCT environment. Applications in the CT scanner demand precalibration to provide acceptable performance.

Keywords Surgical navigation · Electromagnetic tracking · Accuracy analysis · Image-guided therapy · Usability study

Introduction

Real-time tracking of surgical instruments has become an integral part of computer-assisted surgery; it provides guidance to surgeons in complex procedures. Of the several available tracking technologies compatible with medical applications, optical trackers are currently widespread in computer-aided surgical applications. Optical trackers' performance is hardly affected by clinical settings and provide submillimetric measurement accuracy [1–3]. However, continuous line of sight is difficult to maintain due to the considerable number of adjustable instruments present during surgery, such as monitors and lights [4]. Furthermore, only the tracking of large and rigid object is feasible, which is a disadvantage considering the trend to reduce the invasiveness of surgeries.

Electromagnetic (EM) tracking systems are based on the principle of mutual induction, in which a field generator produces a known EM field to localize small EM sensors placed within the tracking volume. EM trackers have gained popularity due to their freedom from line-of-sight restrictions [5–7], small sensor size, and convenience of use [8,9]. In

E. Lugez · H. Sadjadi · G. Fichtinger (✉)
Laboratory for Percutaneous Surgery, School of Computing, Queen's University, Kingston, ON K7L 3N6, Canada
e-mail: fichting@queensu.ca

R. E. Ellis · S. G. Akl
School of Computing, Queen's University, Kingston, ON K7L 3N6, Canada

D. R. Pichora
Departments of Surgery and Mechanical and Materials Engineering, Queen's University, Kingston, ON, Canada

fact, EM sensors can be placed inside the patient's body without having their measurements altered [10]. In addition, as a result of their submillimetric size, sensors can easily be placed inside the tip of needles or surgical instruments [1,5,9,11]. As a result, EM tracking is promising for demanding clinical applications such as endoscopy, orthopedic, and laparoscopic surgeries [12–14]. Nevertheless, EM trackers are susceptible to measurement noise introduced by ferromagnetism and eddy current [4,5,15]. These phenomena are caused by metallic and electrical objects placed in the vicinity of the measurement volume, such as surgical instruments, imaging systems, and monitors. Consequently, depending on the clinical setting, measurement uncertainties may vary considerably [4,6,13], and the specifications provided by the manufacturer might no longer be applicable [3]. This is especially true when surgeries, such as thermal ablation and biopsy procedures, require the use of intraoperative C-arm fluoroscopy [3,12] or CT scanner imaging guidance [10], in which interference in the EM tracked volume is expected [16]. In fact, Krücker et al. [17] reported that it took from one to six CT scans per procedure to verify the placement of inserted electromagnetically tracked needles. Therefore, it is prudent to completely characterize EM trackers for each environment. In addition, measurement accuracy varies with location and angle of the sensor [4,10,18] and need to be differentiated. This work builds upon our preliminary studies [16,19,20], where we discussed the effect of surgical settings on the EM measurement performance. In this work, we further computed the repeatability of the tracker's measurements and calibrated the system in CT environments. We also exhibited the distribution of measurement distortions and determined, using statistical hypothesis tests, that the tracking performance can significantly differ from one environment to another. Our comprehensive assessment has three follow-up applications. First, we can identify optimum setup configurations. Second, we can accurately model and compensate for systematic errors. Third, we can model random errors, not only to report measurement uncertainty, but also to be used in fusion techniques for achieving accurate measurement estimations.

Background and motivations

The manufacturer of the Aurora [Northern Digital, Inc. (NDI), Waterloo, Canada] EM tracking system (EMTS) illustrated the variations of position and orientation measurement performances as a function of translation and rotation in one dimension (1D) in their user guide. However, the error uncertainties provided by the manufacturer may not be representative of the ones encountered in a surgical environment. This is the reason which has led other researchers to assess measurement accuracies of the EM trackers.

Previous attempts in quantifying EM uncertainties are subject to limitations that can be classified in the three following categories.

The first limitation is the coupling of the 3D measurement variables [14,21,22]. Seeberger et al. [21] made use of a resin skull phantom in order to assess the positional accuracy, as a function of coupled translation and orientation, under laboratory and operating room (OR) conditions.

The second limitation is the partial quantification of measurement uncertainties [2–6,12–15,18,21–33], leading to incomplete characterizations as tabulated in Table 1. Unfortunately, these partial quantifications in the literature cannot be combined to provide a comprehensive assessment. This is exemplified by the studies of Maier-Hein et al. and Yaniv et al., who both assessed 5-DOF measurement uncertainties of the planar Aurora system in a metal-free environment. However, reported position measurement accuracy was 0.8 and 1.4 mm, respectively. A cube phantom was employed by Wilson et al. to solely quantify the position accuracy of the Aurora as a function of translation in both a research and clinical environment [6]. The cube phantom was also utilized by Yaniv et al. [3] to quantify the position and orientation accuracy as a function of translation in interventional radiology, CT, and pulmonology suites. Maier-Hein et al. [5] used a translating and rotating mechanism to measure the position accuracy as a function of translation, and the orientation accuracy as a function of a one axis rotation, in a laboratory and CT scanner environment. Another translating and rotating mechanism was employed by Birkfellner et al. [4] to assess the position and orientation accuracies solely as a function of translation in an OR environment. This mechanism was also applied by Hummel et al. [15] in different settings, such as C-arm fluoroscopy, to quantify the positional accuracy in terms of translation, and by Schicho et al. [13] to solely determine the positional accuracy as a function of translation in

Table 1 Comparison of previous studies assessing the 5-DOF measurement accuracy of Aurora systems in undisturbed environments

	Maier-Hein et al. [5]	Yaniv et al. [3]	Hummel et al. [15]	This study
Position				
Translation	0.8	1.4	4.2	0.7
Rotation	NA	NA	3.5	1.3
Orientation				
Translation	NA	2.9	NA	0.8
Rotation	0.9	NA	NA	0.4

Position values are in millimeters, and orientation values are in degrees. Please note that in [15], the Aurora was with a tetrahedral FG, while others used the planar one

"pseudo-realistic OR conditions." Frantz et al. [25] proposed a series of protocols in an undisturbed environment: first a robot arm, second a hemispherical device, which serves to assess coupled position and orientation accuracies, and last a ball-bar device, where sensors are firmly positioned at each end of the device in order to evaluate coupled sensor position and orientation variations relative to the other.

The third limitation follows from introducing additional interference to the uncertainty assessment, such as employing a robot arm in order to move the EM sensor. The metallic and electrical components may create EM field distortion, and mechanical deformation of the arm may add further error to the measurement [10,18,29]. The robot arm protocol was utilized by Shen et al. [10] who, in a first study, quantified the positional accuracy as a function of translation in a CT scanner environment and, in a second study, the positional accuracy as a function of rotation in a CT scanner environment [18].

Earlier studies were limited by coupling translation and rotation displacements, partial assessment, or inexact evaluation. There is a need for a comprehensive study to harmonize earlier EM tracking characterizations in a unified method, reconfirm observations made in different physical environments, and provide solid experimental data for our own operating theater.

Materials and methods

In this study, we prevented any sensor translation while in rotation, or sensor rotation while in translation, in order to independently quantify the variations of position and orientation uncertainties. Plastic scaffolds, whose properties have a negligible effect on the EM field, provided guidance of the sensor to repeatable poses. The presented methods can be adjusted in order to reproduce this protocol with other EM systems (i.e., different tracking volume or sensor size), or other tracking technologies. We conducted the EM measurement uncertainty quantifications on a control, clinical, and a 3D cone beam CT (CBCT) system, as well as in CT scanner environments. The clinical, CBCT, and CT scanner environments were situated in the same OR.

Experimental setup

In this study, we investigated the tracking performance of an alternating current (AC)-based NDI Aurora V2 along with its 5 degrees of freedom (DOF) "FlexCord (Standard)" sensor. According to the manufacturer's specifications, the system provides submillimetric and subdegree measurement accuracies. Moreover, the field generator can transmit magnetic fields over a volume of $500 \times 500 \times 500\,\text{mm}^3$. Further details can be found in [34]. While 6-DOF sensors have the advantage of providing measurements of their roll angle, many computer-assisted procedures employ 5-DOF because of their smaller size [26] when roll angle measurements are not needed.

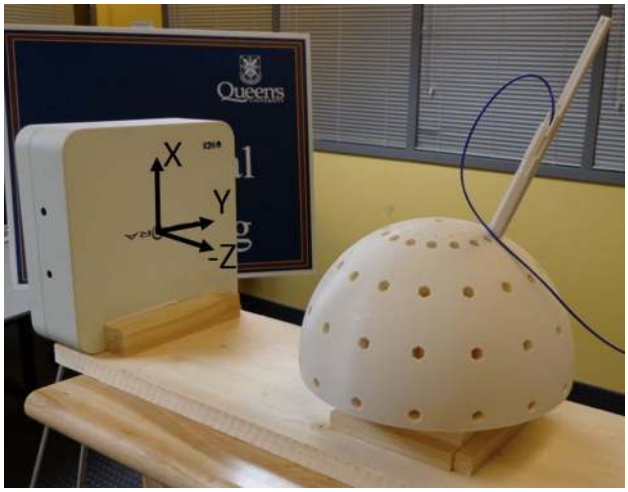

Fig. 1 Control environment. The base, firmly holding the FG (*left*) and a scaffold (*right*), was placed on a wooden table. The global coordinate system is displayed on the FG

To decouple errors due to sensor position from those due to sensor orientation, two repeatability scaffold devices were designed and manufactured by a Dimension SST 1200es (Stratasys, Eden Prairie, USA). The rapid prototyper printed with fast deposition modeling (FDM) using ABSplus thermoplastic material with a resolution of 0.25 mm. The two designed scaffolds enforced constrains in the placement of the sensor; the rotation scaffold ensured the placement of the sensor at a fixed position but at various orientations. The translation scaffold ensured the placement of the sensor at a fixed orientation but at various positions.[1]

The rotation scaffold employs 65 converging paths to study measurement errors caused by rotating the sensor to various orientations without changing the sensor position. The paths are sized to accept a custom plastic inserter in a non-interfering fit (Fig. 1). The inserter, by means of several clips, firmly held and guided the sensor to the exact same position.

The translation scaffold employs 49 parallel paths to study measurement errors caused by translating the sensor to various positions without changing the sensor orientation. The paths are regularly distributed in a $100 \times 100 \times 100\,\text{mm}^3$ volume (Fig. 3).

A measurement base was designed with the following characteristics: First, it firmly held the FG in place. Second, it provided repeatable uncertainty assessments when changing

[1] The scaffolds' STL files will be provided upon request to the corresponding author so that the experiments can be repeated by other groups.

the environment. Third, the scaffolds were in turn inserted into a fitting socket, so that the sensor's pose in the middle path of the translation scaffold coincided with its pose in the top path of the rotation scaffold. In order to evaluate measurement uncertainties in a realistic surgical working volume, the center of each scaffold was located approximately at $X = -50$, $Y = 0$, and $Z = -300$ mm in the EM tracker's global coordinate frame, illustrated in Fig. 1. All further numerical values will also be expressed in this coordinate system. The base was built from wood, whose magnetic permeability is approximately the same as air; hence, the base did not alter either the FG's magnetic field or potential influence from the operating table.

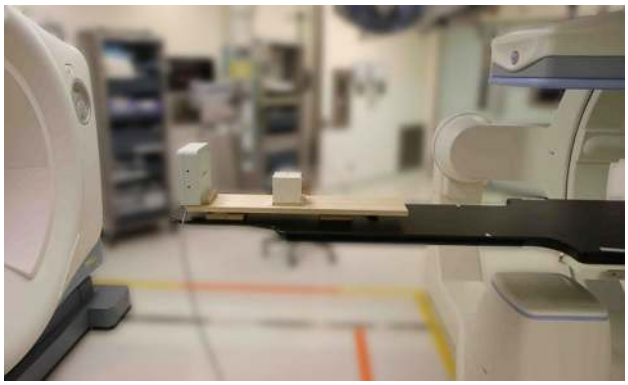

Fig. 2 Clinical environment. The CBCT and CT scanners were placed approximately 1 m away from the FG

Experimental procedure

The EM sensor was manually introduced into each path of the respective scaffolds with an arbitrary orientation around its roll axis. Once inserted to the end of the path, a 10 s data stream of approximately 400 measurement samples was recorded using the NDI Toolbox software. Approximately 570 measurements were collected within the CT environments, due to the pace of the scanner to image the complete working volume.

Control environment In order to provide a baseline for our results, the first experiments were conducted in a control environment. The experimental setup was positioned on a custom-made wooden table which enabled collections of data within a setup free from interference (Fig. 1). No other object was present within 1 m around the FG. Moreover, in this environment, we also assessed the repeatability of the position and orientation measurements by performing fifteen sensor placements in the translation scaffold.

Clinical environment In the clinical environment, the experimental setup was positioned on a carbon-fiber operating table, located midway between a CBCT and a CT scanner (Fig. 2). Separated by a distance of 2 m, the CBCT and CT scanners were fully powered and not emitting X-rays during the entire process of data collection, simulating a surgical setting.

CBCT environment In the CBCT environment, the tracked sensor and scaffolds were placed midway between the source and the receiver of the flat panel fluoroscope (Innova 4100, GE Healthcare, Buc, France), on a carbon-fiber operating table (Fig. 3). For each path, EM tracking uncertainties were studied during X-ray emission from the fluoroscope. In order to determine the potential dynamic distortion from X-rays, measurements were also acquired and compared in three distinct situations: before, during, and after X-ray emission.

CT scanner environment In a CT scanner environment (Fig. 4), the measurement base was placed so that the converging position of the scaffolds' middle path was located in the middle of the CT gantry (Lightspeed+ XCR, General Electric, Milwaukee, USA). In order to evaluate the dynamic distortion caused by the motion or the scanning process of the scanner, three CT conditions were assessed: CT static and not scanning; CT moving (over 100 mm) and not scanning; and CT moving and scanning.

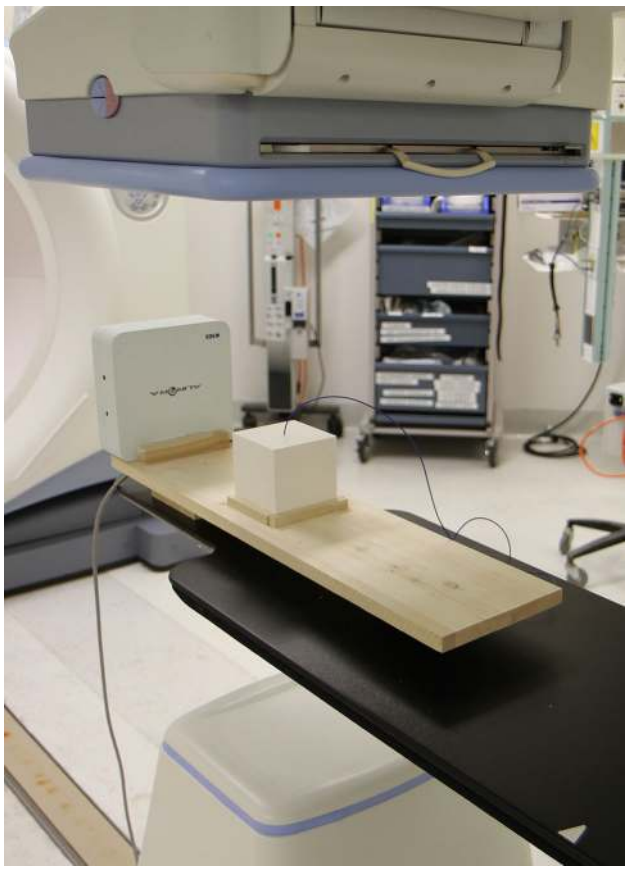

Fig. 3 CBCT environment. The experimental setup was placed midway between the source and the receiver of a CBCT scanner

Fig. 4 CT scanner environment. The experimental setup was placed within a CT scanner gantry

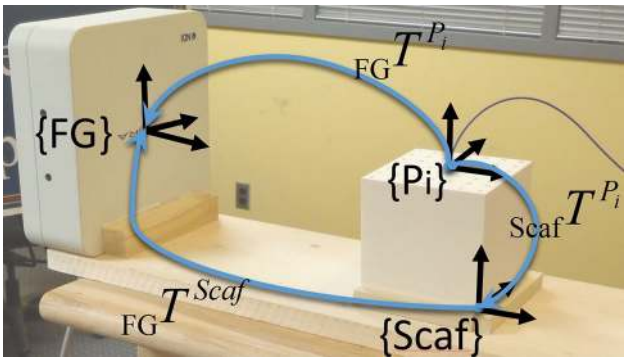

Fig. 5 Coordinate systems and transformations

Tracking performance analysis

Given the known geometry of the scaffold, the transformation ${}_{Scaf}T^{Pi}$ (Fig. 5) from each path i in {Pi} to the scaffold's reference frame $\{Scaf\}$ was computed. In an interference-free environment, the transformations ${}_{\mathrm{FG}}T^{\mathrm{Pi}}$ from $\{Pi\}$ to the EM tracker's reference frame $\{FG\}$ are given by the EM tracking system. ${}_{\mathrm{FG}}T^{Scaf}$ was calculated by rigidly registering ${}_{Scaf}T^{Pi}$ to ${}_{\mathrm{FG}}T^{Pi}$ using Arun's least square method [35]. Arun's rigid registration matched position measurements to their corresponding positions in the scaffold's reference frame. Therefore, the ground truth ${}_{\mathrm{FG}}T^{Pi}$ was computed by ${}_{\mathrm{FG}}T^{Pi} = {}_{\mathrm{FG}}T^{Scaf} \cdot {}_{Scaf}T^{Pi}$ and was used to evaluate the accuracy of the direct measurements ${}_{\mathrm{FG}}T^{Pi}$ by the EM tracker.

The position accuracy Acc_p for each path was determined from the Euclidean distance between the mean measurement position vector $\bar{\mathbf{P}}$ and the corresponding ground truth position vector $\mathbf{P}_{\mathrm{GT}}$. Therefore, Acc_p is defined by the norm: $\mathrm{Acc}_p = \| \mathbf{P}_{\mathrm{GT}} - \bar{\mathbf{P}} \|$.

Sensor's orientation was computed by converting the measured quaternion q, defined as $q = \begin{bmatrix} q_0 & q_1 & q_2 & q_3 \end{bmatrix}^T$, into a rotation matrix R defined as following:

$$R = \begin{bmatrix} 1-2q_2^2-2q_3^2 & 2(q_1q_2-q_0q_3) & 2(q_1q_3+q_0q_2) \\ 2(q_1q_2+q_0q_3) & 1-2q_1^2-2q_3^2 & 2(q_2q_3-q_0q_1) \\ 2(q_1q_3-q_0q_2) & 2(q_2q_3+q_0q_1) & 1-2q_1^2-2q_2^2 \end{bmatrix}$$

The last column of the rotation matrix represents the longitudinal axis of the EM sensor, as defined by the manufacturer. Once the longitudinal axes from a data stream extracted, the average and normalized axis $\bar{\mathbf{A}}$ of the path was computed.

The orientation accuracy Acc_o for each path i was computed as: $\mathrm{Acc}_o = \mathrm{acosd}(\bar{\mathbf{A}}_i \cdot \bar{\mathbf{A}}_{i+1}) - \Psi_{GT}$, with $\mathrm{acosd}(\bar{\mathbf{A}}_i \cdot \bar{\mathbf{A}}_{i+1})$ representing the angle between the axes of two consecutive measured paths $\bar{\mathbf{A}}_i$ and $\bar{\mathbf{A}}_{i+1}$, and Ψ_{GT} representing the corresponding known ground truth angle.

The position precision σ_p for each path was defined as the standard deviation of all the measurements $\mathbf{P}_{\mathrm{j}}$, with $j = 1, 2, \ldots, N$ and N the number of measurements recorded in the data stream. Therefore, the position precision was: $\sigma_p = \sqrt{\frac{1}{N}\sum_{j=1}^{N}(\mathbf{P}_{\mathrm{j}} - \bar{\mathbf{P}})^2}$.

Similarly, the orientation precision σ_o for each path was computed based on the standard deviation of all the measurements of sensor axes $\mathbf{A}_{\mathrm{j}}$. Therefore, $\sigma_o = \sqrt{\frac{1}{N}\sum_{j=1}^{N}(\mathrm{acosd}(\mathbf{A}_{\mathrm{j}} \cdot \bar{\mathbf{A}}))^2}$.

Data were assembled into four categories: position statistics as the sensor was translated within the translation scaffold; position statistics as the sensor was rotated within the rotation scaffold; orientation statistics during translation within the translation scaffold; orientation statistics during rotation within the rotation scaffold.

For the CT scanner environment where substantial tracking error is expected, a static preoperative calibration was performed to compensate for the tracking errors due to high magnetic field distortion. For that, we first collected the data for calibration as explained in "Experimental procedure" section for several gantry positions over the measurement volume in the CT scanner. Second, we computed the mean measurement error $\mathbf{E}$ for each path of the two scaffolds, where each column of $\mathbf{E}$ corresponded to the error in each DOF (X, Y, Z, q_0, q_1, q_2). Note that $q_3 = 0$ because the roll angle was not measured. Third, we employed a custom Matlab code to model the tracking errors with a fourth-order polynomial [36]. For example, the nth degree of freedom measurement error was modeled as a function of measurement pose (X, Y, Z, q_0, q_1, q_2):

$$\mathbf{E}_n = \sum_{j=1}^{K} (cp_{n,j} \cdot X^{s_j} Y^{t_j} Z^{u_j} + cq_{n,j} \cdot q_0^{s_j} q_1^{t_j} q_2^{u_j}),$$

where $K = 35$ is the number of coefficients required for the fourth-order polynomial fitting and s_j, t_j, u_j are the nonnegative powers such that $0 \leq s_j + t_j + u_j \leq 4$ and all the permutations of $\{s_j, t_j, u_j\}$ are unique. cp and cq, computed from the calibration data, were used to compensate the measurement errors. For further details about this technique, please refer to the works of Ikits et al. [36] and Kindratenko [37].

The root-mean-square (RMS) accuracies, 95 % confidence intervals (CI), and the RMS precisions of the tracker in each environment were found. Note that the system control unit of the Aurora did not return any measurement for particular sensor poses in the CT environment due to substantial field distortions. These non-visible paths were therefore not considered in the uncertainty assessment. As a result, RMS accuracies and precisions reflect successful measurements returned by the tracking system. Finally, paired-sample t tests—or two-sample t tests when the size of the data sets differed—were computed to compare the environments.

Results

Measurement uncertainties from the different environments are tabulated in Table 2, and further represented as box plots in Fig. 6. In the control environment, RMS position and orientation measurement repeatabilities were 0.4 mm and 0.9°, respectively, and tracking accuracies were similar to the corresponding values reported by the manufacturer. The clinical environment was slightly more distorted due to the surrounding equipment. Within the 3D CBCT environment, tracking errors were on average three times higher than under the control setting. The most distorted environment was the CT scanner, with an average tracking error twelve times higher than the control one. Indeed, many of the paths pointing toward the FG could not be sensed by the EMTS in the CT environment.

Increased measurement errors were observed when the sensor was positioned toward the extremities of the measurement volume, as illustrated in Fig. 7, and when inserted in deeper paths. Furthermore, the highest accuracy errors were detected when the sensor was oriented closer to the Z axis (longitudinal axis of the FG), both pointing away or toward from the FG.

Tracking precision is characterized in Fig. 7. In order to fit into the graph, deviations within the CT scanner were plotted with a lower scaling factor. Sensor readings were repeatedly found to be spread out along the Z axis. In our setups, we observed that the more the environment was distorted, the more this precision pattern was pronounced. In fact, within the CT scanner, distortion along the Z axis was approximately twice as high as those along the X and Y axes.

CBCT imaging influence on uncertainties The measurement uncertainties were not significantly influenced by X-ray fluoroscopy ($0.4 \leq t < 2.0$, $0.06 \leq p \leq 0.7$). Equivalent accuracy distributions were observed throughout the three X-ray situations.

Dynamic effects of CT motions and scanning As tabulated in Table 2, consistent results throughout the three CT conditions were observed. Position measurement accuracies as a function of translation and rotation were not significantly different whether or not the CT was moving or scanning. This implies that static errors predominated over the potential dynamic errors. Conversely, orientation measurement accuracies as a function of translation significantly differed whether the CT was in motion or not ($t(32) = 2.6$, $p = 0.01$). This implies that the motion of the CT scanner had significantly introduced dynamic errors to the orientation measurements as a function of translation.

Table 2 Accuracies and precisions of the Aurora tracker within a control, a clinical, a CBCT, and CT scanner environments

			Control	Clinical	CBCT	CT static	CT moving	
						X-ray off	X-ray off	X-ray on
Position	Translation	Accuracy RMS	0.7	1.4	3.2	5.2	5.1	5.0
		Precision RMS	0.1	0.1	0.2	0.1	0.6	1.7
		Accuracy 95 CI	1.2	2.2	4.6	8.2	9.5	8.4
	Rotation	Accuracy RMS	1.3	1.2	4.0	25.4	27.0	26.9
		Precision RMS	0.1	0.3	0.1	0.1	3.2	1.9
		Accuracy 95 CI	1.8	1.9	8.2	36.0	45.0	38.6
Orientation	Translation	Accuracy RMS	0.8	0.8	1.6	1.7	2.0	1.9
		Precision RMS	0.0	0.0	0.0	0.0	0.0	0.2
		Accuracy 95 CI	1.3	1.3	3.1	2.9	3.0	3.1
	Rotation	Accuracy RMS	0.4	1.0	1.7	5.2	5.8	5.7
		Precision RMS	0.1	0.1	0.5	0.0	0.2	0.3
		Accuracy 95 CI	1.5	2.1	3.4	8.2	9.7	6.9

Position values are in millimeters, and orientation values are in degrees

Calibration of tracking measurements within CT scanner Tabulated in Table 3, the calibration improved the average measurement accuracies by 50–85 %. Improved accuracies were observed when the sensor was maintained with a constant angle.

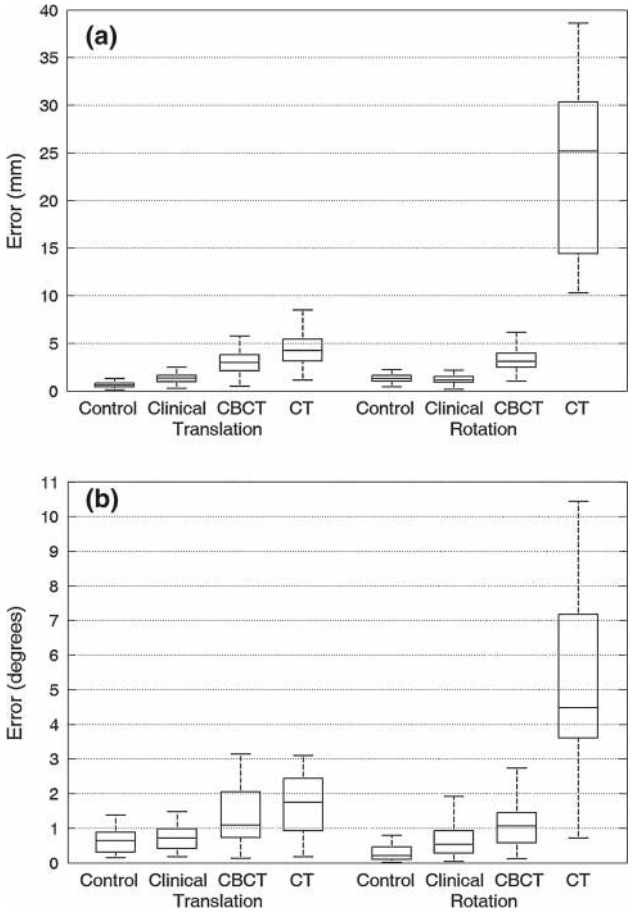

Fig. 6 Position (**a**) and orientation (**b**) measurement errors within the assessed environments. The *box plots* display the EMTS characteristics (median, 25th and 75th percentiles, and extreme non-outlying errors) as a function of translation (*left-sided box plots*) and rotation (*right-sided box plots*)

Discussions

EM tracking has become promising for demanding surgical applications owing to its small sensor size and no line-of-sight restrictions. Nevertheless, its performance may vary depending on the surrounding environment and sensor pose. Tracking performance variations of an Aurora system were assessed as the sensor was translated and then rotated within a control, a clinical, a 3D CBCT, as well as CT scanner environments.

Position measurement accuracy and precision varied as a function of sensor translation and rotation. In fact, at a fixed sensor position in the clinical environment, the systematic measurement error changed from 0.2 to 2.2 mm depending on the sensor orientation. The disparity of measurement accuracies whether the sensor was translated or rotated (position measurement error within the CT scanner was 5.0 mm during translation vs. 26.9 mm during rotation) showed the importance of characterizing both position and orientation measurement errors as a function of both sensor translation and rotation, in order to optimize the setup and the correction of systematic errors. Lower position measurement accuracy was observed when the sensor was translated toward the edges of the measured volume and when the insertion depth increased. This pattern may be explained by the fact that the center of the scaffold's measurement volume was placed at the most efficient tracking location. As a result, the more the sensor was moved away from the efficient location, the more the tracking performance decreased. Compared to the baseline results, position errors were double in the clinical environment, six times higher within the CBCT setting, and twelve times higher within the CT scanner environment, confirming previous studies [4,5,15].

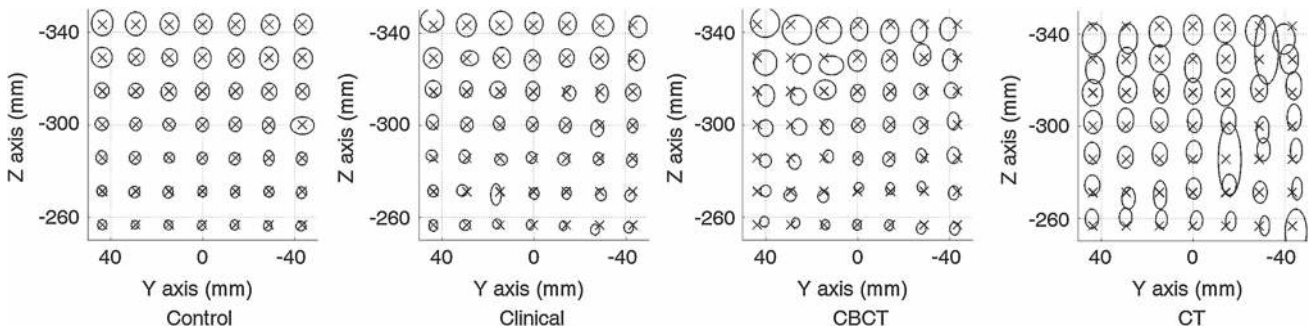

Fig. 7 Precision of the position measurements as a function of translation within the assessed environments. The *crosses* represent the ground truth position. The *ellipses*, *centered* on the corresponding mean position measurement, represent the scaled precision. For the CT environment, ellipses are scaled down 20 times compared to the ones in other environments

Table 3 Accuracies of the calibrated measurements under three CT conditions

			CT static	CT moving	
			X-ray off	X-ray off	X-ray on
Position	Translation	Accuracy RMS	1.5	2.5	2.5
		Accuracy 95 CI	2.6	4.0	4.2
	Rotation	Accuracy RMS	3.6	3.5	4.8
		Accuracy 95 CI	6.3	5.5	8.6
Orientation	Translation	Accuracy RMS	0.9	0.7	0.7
		Accuracy 95 CI	1.7	1.1	1.1
	Rotation	Accuracy RMS	2.1	1.7	3.1
		Accuracy 95 CI	2.7	4.9	4.9

Values are in millimeters and degrees

Similarly, orientation measurement accuracy was improved when the sensor was oriented along the vertical axis of the FG. Furthermore, we noticed that the paths oriented along the FG longitudinal axis, and pointing away or toward the FG, always had diminished performance in every environment. While this pattern may be caused by some printing default, the resolution of the used 3D printer was approximately 0.25 mm. Nevertheless, the accuracy errors measured in the control environment were extremely low, even for this altered path. This involved having the 3D printings accurately printed from the sketch drawings. In order for us to be even more convinced about this eventual printing default, we rotated the scaffold 90 degrees within the base. We found similar results compared to the earlier ones and confirmed the pattern. Compared to the baseline results, orientation errors were double in the clinical environment, four times higher within the CBCT setting, as well as fourteen times higher within the CT scanner environment. Although it is not surprising that the properties of the surrounding environment have a major effect on tracking uncertainties, we noticed that within the CT gantry, many of the paths were not visible by the Aurora system.

Accordingly, the Aurora device is adequate for a variety of surgical procedures, such as pedicle screw insertion [38] or tumor therapy [39], within a clinical environment. Although higher measurement errors were observed within the CBCT scanner, equivalent accuracy distributions were obtained when the experiments were repeated. Consequently, errors are systematic and can be minimized using a high-order polynomial fit or other correction schemes. In addition, EM tracking can still provide valuable assistance to procedures within a CT scanner environment, such as lung or other tissue biopsies [39] and may reduce the number of verification scans needed to validate the placement of surgical instruments, such as needles for percutaneous interventions. The errors found in these experiments are lower than those found by Yaniv et al. [3], who studied the position and rotation measurement errors during sensor translation. Nevertheless, Yaniv et al. [3] concluded that the Aurora system was accurate enough for their purposes, in particular for thoracic–abdominal procedures. Maier-Hein et al. [5] found that other available EM systems could be more accurate and robust than the Aurora, in close proximity of a CT scanner.

Although the measurement accuracies can be improved, the tracker's visibility issues in the CT environments remain a challenge. Multimodal or monomodal sensor fusion using Kalman filters [7–9] may temporarily compensate for the failures of tracking visibility and improve the measurement quality, while maintaining the advantages of EM tracking.

This work primarily described the assessment procedure for characterizing the static measurement error. This can help compare the impact of various environments on tracking error and decide whether the EM tracking technology is appropriate for a specific procedure. In other words, if static tracking errors are superior to the application's requirements, EM technology may not be suitable. There are also additional tracking errors that are introduced depending on the dynamic nature of the application. For example, sampling rate and measurement latency are important elements to consider. It was shown that sampling rate of 25–30 Hz is adequate for navigation with a human operator, while higher sampling rates may be required when navigation is operated robotically [3]. Navigation speed is another important element to consider. The majority of procedures involve careful and slow motions of instruments due to patient safety, and they can be considered quasi-static. However, for fast motions, the undesired dynamic errors may be noticeable and can be minimized via statistical filtering [37], such as Kalman filters. In fact, this study is a necessary step for the modeling of random measurement errors used in Kalman filters.

Conclusions

A complete characterization of the EM tracking system is necessary whether it is used for sole tracking assistance or

combined with another tracking technology. This paper presented comprehensive and consistent assessments of the NDI Aurora tracking accuracy and precision by means of a simple, reliable, and highly repeatable method. Improved measurement accuracies were observed when the sensor was held along the vertical axis of the FG. In practice, it is recommended to align this axis in the direction where the most motion is expected. We observed that EM tracking within a clinical environment provides satisfactory measurements for a variety of potential surgical procedures. Tracking errors within the CBCT environment were systematic and therefore can be minimized. In fact, we did not find significant influence ($0.06 \leq p \leq 0.7$) on the EM tracking performance from X-ray fluoroscopy using the CBCT scanner. EM tracking is therefore promising for surgeries that may require the use of a CBCT, in combination with an error minimization method. While tracking within a CT scanner gantry is difficult, dynamic errors introduced by the motion and scanning process of the scanner were not significant compared to the inherent influence of the CT scanner itself. The implemented calibration improved by 50–85 % the measurement accuracy of the tracking system, becoming sufficiently accurate for many surgical procedures. EM tracking appears to be a convenient tool for use in a variety of surgical navigation systems.

Acknowledgments The authors would like to thank Dr. Abdulaziz Al Qahtani, clinical fellow, for his assistance in collecting data. This work was supported by the Natural Sciences and Engineering Research Council of Canada, and the Canada Foundation for Innovation. Gabor Fichtinger was supported as Cancer Care Ontario Research Chair.

Conflict of interest Elodie Lugez, Hossein Sadjadi, David Pichora, Randy Ellis, and Gabor Fichtinger declare that they have no conflict of interest.

References

1. Thompson S, Penney G, Dasguta P, Hawkes D (2013) Improved modelling of tool tracking errors by modelling dependent marker errors. IEEE Trans Med Imaging 32:165
2. Kwartowitz DM, Rettmann ME, Holmes III DR, and Robb RA (2010) A novel technique for analysis of accuracy of magnetic tracking systems used in image guided surgery. In: Proc SPIE, pp 76251L–76251L. International Society for Optics and Photonics
3. Yaniv Z, Wilson E, Lindisch D, Cleary K (2009) Electromagnetic tracking in the clinical environment. Med Phys 36:876
4. Birkfellner W, Watzinger F, Wanschitz F, Enislidis G, Kollmann C, Rafolt D, Nowotny R, Ewers R, Bergmann H (1998) Systematic distortions in magnetic position digitizers. Med Phys 25:2242
5. Maier-Hein L, Franz AM, Birkfellner W, Hummel J, Gergel I, Wegner I, Meinzer H-P (2012) Standardized assessment of new electromagnetic field generators in an interventional radiology setting. Med Phys 39:3424
6. Wilson E, Yaniv Z, Zhang H, Nafis C, Shen E, Shechter G, Wiles AD, Peters T, Lindisch D and Cleary K(2007) A hardware and software protocol for the evaluation of electromagnetic tracker accuracy in the clinical environment: a multi-center study. In: Proc SPIE, pp 65092T–65092T. International Society for Optics and Photonics
7. Sadjadi H, Hashtrudi-Zaad K and Fichtinger G (2014) Needle deflection estimation: prostate brachytherapy phantom experiments. Int J CARS. doi:10.1007/s11548-014-0985-0
8. Sadjadi H, Hashtrudi-Zaad K, Fichtinger G (2013) Fusion of electromagnetic trackers to improve needle deflection estimation: simulation study. IEEE Trans Biomed Eng 60:2706–2715
9. Sadjadi H, Hashtrudi-Zaad K and Fichtinger G (2012) Needle deflection estimation using fusion of electromagnetic trackers. In: 2012 annual international conference of the IEEE engineering in medicine and biology society (EMBC). IEEE, pp 952–955
10. Shen E, Shechter G, Kruecker J, Stanton D (2007) Quantification of ac electromagnetic tracking system accuracy in a ct scanner environment. In: Proc SPIE. International Society for Optics and Photonics, pp 65090L–65090L
11. Cleary K, Zhang H, Glossop N, Levy E, Wood B and Banovac F (2005) Electromagnetic tracking for image-guided abdominal procedures: Overall system and technical issues. In: 27th Annual international conference of the engineering in medicine and biology society, 2005. IEEE-EMBS 2005. IEEE, pp 6748–6753
12. Bo LE, Leira HO, Tangen GA, Hofstad EF, Amundsen T, Lango T (2012) Accuracy of electromagnetic tracking with a prototype field generator in an interventional or setting. Med Phys 39(1):399
13. Schicho K, Figl M, Donat M, Birkfellner W, Seemann R, Wagner A, Bergmann H, Ewers R (2005) Stability of miniature electromagnetic tracking systems. Phys Med Biol 50(9):2089
14. Feuerstein M, Reichl T, Vogel J, Traub J, Navab N (2009) Magneto-optical tracking of flexible laparoscopic ultrasound: Model-based online detection and correction of magnetic tracking errors. IEEE Trans Med Imaging 28(6):951–967
15. Hummel J, Figl M, Kollmann C, Bergmann H, Birkfellner W (2002) Evaluation of a miniature electromagnetic position tracker. Med Phys 29:2205
16. Lugez E, Pichora D, Akl S, Ellis R (2014) Intraoperative ct scanning impact on electromagnetic tracking performance. Int J CARS 9(Suppl 1):S107–S108
17. Krücker J, Xu S, Glossop N, Viswanathan A, Borgert J, Schulz H, Wood BJ (2007) Electromagnetic tracking for thermal ablation and biopsy guidance: clinical evaluation of spatial accuracy. J Vasc Interv Radiol 18(9):1141–1150
18. Shen E, Shechter G, Kruecker J and Stanton D (2008) Effects of sensor orientation on ac electromagnetic tracking system accuracy in a ct scanner environment. In: Proceedings of SPIE, vol 6918, pp 691823
19. Lugez E, Pichora D, Akl S, Ellis R (2013) Accuracy of electromagnetic tracking in an operating-room setting. Int J CARS 8(Suppl 1):S147–S148
20. Lugez E, Pichora DR, Akl SG, and Ellis RE (2013) Accuracy of electromagnetic tracking in an image-guided surgery suite. Int Bone Joint J, 95-B(Supp 28):25–25
21. Seeberger R, Kane G, Hoffmann J, Eggers G (2012) Accuracy assessment for navigated maxillo-facial surgery using an electromagnetic tracking device. J Cranio Maxill Surg 40(2):156–161
22. Kral F, Puschban EJ, Riechelmann H, Freysinger W (2013) Comparison of optical and electromagnetic tracking for navigated lateral skull base surgery. Int J Med Robot Comp 9:247–252
23. Atuegwu NC, Galloway RL (2008) Volumetric characterization of the aurora magnetic tracker system for image-guided transorbital endoscopic procedures. Phys Med Biol 53(16):4355
24. Day JS, Murdoch DJ, Dumas GA (2000) Calibration of position and angular data from a magnetic tracking device. J Biomech 33(8):1039–1045
25. Frantz DD, Wiles AD, Leis SE, Kirsch SR (2003) Accuracy assessment protocols for electromagnetic tracking systems. Phys Med Biol 48(14):2241

26. Franz AM, März J, Hummel J, Birkfellner W, Bendl R, Delorme S, Schlemmer H-P, Meinzer H-P, Maier-Hein L (2012) Electromagnetic tracking for us-guided interventions: standardized assessment of a new compact field generator. Int J Comput Assist Radiol. Surg 7(6):813–818
27. Hummel JB, Bax MR, Figl ML, Kang Y, Maurer C, Birkfellner WW, Bergmann H, Shahidi R (2005) Design and application of an assessment protocol for electromagnetic tracking systems. Med Phys 32:2371–2379
28. LaScalza S, Arico J, Hughes R (2003) Effect of metal and sampling rate on accuracy of flock of birds electromagnetic tracking system. J Biomech 36:141–144
29. Milne AD, Chess DG, Johnson JA, King GJW (1996) Accuracy of an electromagnetic tracking device: a study of the optimal operating range and metal interference. J Biomech 29(6):791–793
30. Poulin F, Amiot L-P (2002) Interference during the use of an electromagnetic tracking system under or conditions. J Biomech 35(6):733–737
31. Stevens F, Kulkarni N, Ismaily SK, Lionberger DR (2010) Minimizing electromagnetic interference from surgical instruments on electromagnetic surgical navigation. Clin Orthop Relat Res 468(8):2244–2250
32. Wagner A, Schicho K, Birkfellner W, Figl M, Seemann R, König F, Kainberger F, Ewers R (2002) Quantitative analysis of factors affecting intraoperative precision and stability of optoelectronic and electromagnetic tracking systems. Med Phys 29:905
33. Wegner I, Teber D, Hadaschik B, Pahernik S, Hohenfellner M, Meinzer H-P, Huber J (2012) Pitfalls of electromagnetic tracking in clinical routine using multiple or adjacent sensors. Int J Med Robot Comp 9:268–273
34. http://www.ndigital.com/medical/products/aurora/
35. Arun KS, Huang TS and Blostein SD (1987) Least-squares fitting of two 3-d point sets. IEEE Trans Pattern Anal Mach Intell, PAMI-9:698–700
36. Ikits M, Brederson JD, Hansen CD and Hollerbach JM (2001) An improved calibration framework for electromagnetic tracking devices. In: Proceedings of the IEEE virtual reality. IEEE, pp 63–70
37. Kindratenko V (2000) A survey of electromagnetic position tracker calibration techniques. Virtual Real 5(3):169–182
38. Rampersaud YR, Simon DA, Foley KT (2001) Accuracy requirements for image-guided spinal pedicle screw placement. Spine 26(4):352–359
39. Liu J, Zhang Y, Li Z (2007) Improving the positioning accuracy of a neurosurgical robot system. IEEE/ASME Trans Mechatron 12(5):527–533